Theoretical Study of the Intercalation of Li into TiO_2 Structures

Ľubomír Benco,*,† Jean-Luc Barras, and Claude Auguste Daul

Institute of Inorganic Chemistry, University of Fribourg, Pérolles, CH-1700 Fribourg, Switzerland

Erich Deiss

Department of General Energy Research, Paul Scherrer Institute, CH-5232 Villigen, Switzerland

Received March 27, 1998

First principles LAPW and semiempirical EHT methodology is used to characterize the bonding in $LiTi_2O_4$ (spinel) and $LiTiO_2$ (trigonal) as well as the corresponding Li-extracted TiO_2 structures. In optimized structures, the Ti−Ti distance indicates that the spinel structure is most stable, in agreement with experimental observations. Deintercalated compounds of both structures are broad-band insulators with a gap of ∼2 eV. Upon intercalation of Li both structures become conductors with the Fermi level situated within the d band. The intercalation causes no pronounced changes of the DOS of cubic spinels. On the contrary, trigonal compounds show considerable rearrangement of energy states at the bottom of the d band. Both, density of states and difference density plots show that the host framework of TiO_2 oxide becomes more ionic with intercalation of Li. The interaction scheme constructed for spinel structures shows that electron density originating from intercalated Li atoms can be placed only on Ti atoms, which is confirmed by electron density plots. The difference density plots constructed for Li electron density only show that the occupation of d states due to the intercalation creates Ti−Ti (t_{2g}−t_{2g}) bonds in a more effective manner in the spinel than in the trigonal structure. This 3D t_{2g} band is the electronic prerequisite for the superconductivity of the spinel $LiTi_2O_4$ compounds.

1. Introduction

Oxides of transition metals (TM) are potential materials for the intercalation of Li and its usage in rechargable Li batteries.[1] In higher oxidation states, their structures are open enough to afford high Li diffusivity, and TMs have the capacity to accommodate the electron density contributed by Li atoms. For good ionic conductivity the interstitial space must be interconnected throughout the structure giving rise to a relatively smooth potential energy surface for the mobile Li ions. Fourth period TMs form two kinds of structures with Li meeting these criteria: (i) cubic spinels with 3D networks of the interconnected interstitial space, and (ii) trigonal layered structures (e.g. α-$NaFeO_2$).[2] Both crystal structures are shown in Figure 1. While the spinel structure is typical for fourth period TMs on the left side of the periodic table (Ti,[3−6] Mn[7,8]). Fourth period TMs on the right side of the periodic table rather form stable layered structures (Co,[9] Ni[10]). Vanadium is stable in both spinel[11−13] and layered[14,15] structures.

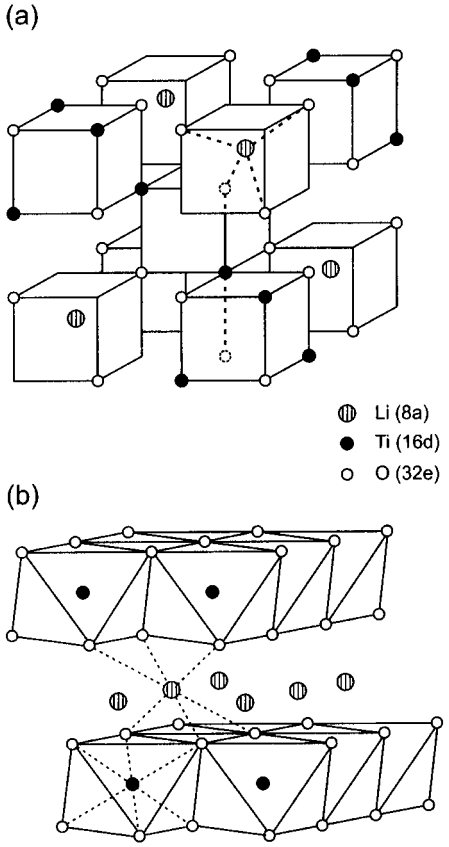

Figure 1. Sketches of structures: (a) cubic spinel structure of $LiTi_2O_4$, (b) layered trigonal structure of $LiTiO_2$.

* Address for correspondence: Institute of Theoretical Physics, Vienna University of Technology, Wiedner Hauptstrasse 8-10/136, A-1040 Vienna, Austria.

† Permanent address: Institute of Inorganic Chemistry, Slovak Academy of Sciences, Dúbravská cesta 9, SK-84236 Bratislava, Slovakia.

(1) Pistoia, G. (Ed.) *Lithium Batteries*; Elsevier: Amsterdam, 1994.
(2) Wells, A. F. *Structural Inorganic Chemistry*; Clarendon: Oxford, 1984.
(3) Deschanvres, A.; Raveau, B.; Sekkal, Z. *Mater. Res. Bull.* **1971**, *6*, 699.
(4) Cava, J. R.; Murphy, D. W.; Zahurak, S. *J. Solid State Chem.* **1984**, *53*, 64.
(5) Akimoto, J.; Gotoh, Y.; Kawaguchi, K.; Oosawa, Y. *J. Solid State Chem.* **1992**, *96*, 446.
(6) Campá, J. A.; Vélez, M.; Cascales, C.; Gutiérrez Puebla, E.; Monge, M. A. *J. Crystal Growth* **1994**, *142*, 87.
(7) Fong, C.; Kennedy, B. J.; Elcombe, M. M. *Z. Kristallogr.* **1994**, *209*, 941.
(8) Thackeray, M. M.; de Kock, A.; David, W. I. F. *Mater. Res. Bull.* **1993**, *28*, 1041.

10.1021/ic9803558 CCC: $18.00
Published on Web 12/11/1998

Efforts to characterize the properties of Li intercalation compounds using the tools of theoretical chemistry have focused on (i) the investigation of the bonding, (ii) the calculation of the average cell voltages, and (iii) a description of diffusion within the solid electrode. Although much work has been done to characterize transport phenomena on a macroscopic level,[16] an up-to-date Carr−Parinello-type molecular dynamics applications[17] are still missing.

The electronic structure of Li intercalated compounds has been studied using a variety of methods. Both semiempirical[18] and first principles approaches[19−24] have been applied. Most of these studies were aimed at characterizing the bonding within the host TM compound and the influence of the intercalated Li atom on the electronic structure. There is general agreement that the bonding of Li with the surrounding nonmetal atoms is highly ionic. However the position of the Fermi level (E_F) has been discussed at length. The position of E_F determines the electronic conductivity, which is a very important property for electrode materials. The intercalation of Li, adding Li valence electron density to the valence bonding band, drives E_F into another position, thus influencing the conducting properties. A direct comparison of calculated E_F values with those obtained from experimental procedures is usually not possible. The shape of the density of states (DOS) and the position of E_F within the DOS is correct and comparable to those derived from experimental data.[25,26] The position of the DOS on the energy scale, however, is arbitrary. This is due to numerical approximation of the core states in the pseudopotential method or because of the description of the potential acting on electrons between spheres in the LAPW method.

Another difficulty for the comparison of bonding in different electrode materials is the absence of the energy gap. Most of the materials under study are conductors without energy gap showing considerable mixing of states in the vicinity of E_F. When intercalation takes place the electron density from Li fills empty electronic states above E_F and complex bonding properties result which prevent a straightforward reasoning about the role of Li atoms.

In this paper we present crystal−orbital calculations to study the intercalation of Li into TiO_2. A great advantage for our analysis is the simple electronic configuration of TiO_2. Stoichiometric TiO_2 has closed shells with a completely filled p band separated from the empty d band by a sizable energy gap for all structure modifications.[27] First we present the full geometry optimization of the intercalated and deintercalated TiO_2 structures in both spinel and layered structure modifications. Then we focus on the bonding properties investigated by means of total and partial DOS. Based on atomic energy levels and orbital interactions indicated by the partial DOS we have constructed the interaction schemes. Interaction schemes have been successfully applied to various bonding situations[28−31] and were demonstrated to be a useful tool for displaying essential bonding characteristics of a solid in one simple figure. Such schemes are then compared for intercalated and deintercalated systems. Finally, we present our evaluation of the bonding properties in terms of crystal orbital overlap population curves and in terms of electron density maps constructed for equivalent cutting planes. The modification of the electron density due to the bonding is displayed in terms of the difference density maps. The distribution of the additional electron density originating from intercalated Li atoms is displayed by means of the difference band density, showing the transfer of electron density from the Li atoms to the framework of the TM oxide.

2. Method

The electronic and structural properties of the compounds were calculated within the framework of periodical, three-dimensional crystal orbital (CO) calculations by solving the Kohn−Sham (KS) equations[32] within the linearized augmented plane wave (LAPW) approximation.[33−35] We used the all-electron full-potential version of the LAPW method as implemented in WIEN97 code.[36] Core states were treated fully relativistically[37] and for valence states relativistic effects were included in a scalar relativistic treatment.[38] The exchange and correlation effects are treated beyond the LDA by adding gradient dependent terms of the electron density to the energy and its corresponding potential terms (i.e., the generalized-gradient approximation: GGA[39]). The maximum l value in the expansion of the basis set inside atomic spheres was 8 and 4 for the computation of muffin-tin and nonmuffin-tin matrix elements, respectively. A grid of 781 points on a logarithmic scale was chosen for the evaluation of functions inside atomic spheres. The parameter $R_{mt}K_{max} = 8$ (where R_{mt} is the smallest atomic sphere radius in the unit cell and K_{max} is the magnitude of the largest K vector) led to an energy cutoff of $E_{cut} \approx 27$ Ry for the expansion of plane waves to complete the basis set with functions for the interstitial region. Performing the structure optimization we have used the set of 4 **k** points for the cubic and 19 **k** points for the trigonal structure (for a description of structures see below). Electronic properties within optimal structures were evaluated using a set of 35 **k** points in the irreducible wedge of the face-centered cubic Brillouin zone (BZ) and using a set of 65 **k** points in the trigonal BZ. The self-consistency was typically reached in 10 iterations, when the total energy was stable to within 0.1 mRy between two iterations.

The population analysis was performed using the extended Hückel tight-binding semiempirical calculations.[40,41] The atomic parameters used are listed in Table 1.

(9) Ohzuku, T.; Ueda, A.; Nagayama, M.; Iwakoshi, Y.; Komori, H. *Electrochim. Acta* **1993**, *38*, 1159.
(10) Dyer, L. D.; Borie, B. S.; Smith, G. P. *J. Am. Chem. Soc.* **1954**, *76*, 1499.
(11) Pollert, E. *Kristall und Technik* **1973**, *8*, 859.
(12) Chieh, C.; Chamberland, B. L.; Wells, A. F. *Acta Crystallogr.* **1981**, *37*, 1813.
(13) Picciotto, L. A.; Thackeray, M. M. *Mater. Res. Bull.* **1985**, *20*, 187.
(14) Ruedorff, W.; Becker, H. *Z. Naturforsch.* **1954**, *B9*, 614.
(15) Cardoso, L. P.; Cox, D. E.; Hewston, T. A.; Chamberland, B. L. *J. Solid State Chem.* **1988**, *72*, 234.
(16) Newman, J. S. *Electrochemical Systems*; Prentice Hall: Englewood Cliffs, NJ, 1991.
(17) Carr, R.; Parinello, M. *Phys. Rev. Lett.* **1985**, *55*, 2471.
(18) McCanny, J. V. *J. Phys.* **1979**, *C12*, 3263.
(19) Umrigar, C.; Ellis, D. E.; Wang, D.-S.; Krakauer, H.; Posternak, M. *Phys. Rev.* **1982**, *B26*, 4935.
(20) Gou, G. Y.; Liang, W. Y. *J. Phys.* **1987**, *C20*, 4315.
(21) Miura, M.; Yamada, A.; Tanaka, M. *Electrochim. Acta* **1995**, *41*, 249.
(22) Aydinol, M. K.; Ceder, G. *J. Electrochem. Soc.* **1997**, *144*, 3832.
(23) Aydinol, M. K.; Kohan, A. F.; Ceder, G.; Cho, K.; Joannopoulos, J. *Phys. Rev.* **1997**, *B56*, 1354.
(24) Ceder, G.; Aydinol, M. K.; Kohan, A. F. *Comput. Mater. Sci.* **1997**, *8*, 161.
(25) Grunes, L. A.; Leapman, R. D.; Wilker, C. N.; Hoffmann, R.; Kunz, A. B. *Phys. Rev.* **1982**, *B25*, 7157.
(26) Glassford, K. M.; Chelikowsky, J. R. *Phys. Rev.* **1992**, *B46*, 1284.
(27) Cox, P. A. *Transition Metal Oxides*; Clarendon: Oxford, 1992.
(28) Benco, Ľ. *Solid State Commun.* **1995**, *94*, 861.
(29) Benco, Ľ. *J. Solid State Chem.* **1997**, *128*, 121.
(30) Benco, Ľ. *Ceram. Int.* **1998**, *24*, 333.
(31) Dudešek, P.; Benco, Ľ. *J. Am. Ceram. Soc.* **1998**, *81*, 1248.
(32) Kohn, W.; Sham, L. J. *Phys. Rev.* **1965**, *140*, A1133.
(33) Koelling, D. D.; Arbman, G. O. *J. Phys.* **1975**, *F5*, 2041.
(34) Andersen, O. K. *Phys. Rev.* **1975**, *B12*, 3060.
(35) Singh, D. *Plane Waves, Pseudopotentials and the LAPW Method*; Kluwer Academic: Amsterdam, 1994.
(36) Blaha, P.; Schwarz, K.; Luitz, J. *Wien97*; Vienna University of Technology: Vienna, 1997.
(37) Descalaux, J. P. *Comput. Phys. Commun.* **1969**, *216*, 1.
(38) Koelling, D. D.; Harmon, B. N. *J. Phys. C.: Solid State Phys.* **1977**, *10*, 3107.
(39) Perdew, J. P.; Wang, Y. *Phys. Rev.* **1992**, *B45*, 13244.
(40) Hoffmann, R. *Rev. Mod. Phys.* **1988**, *60*, 601.

Table 1. Orbital Parameters Used in Semiempirical Band-Structure Calculations[a]

atom	orbital	H_{ii} (eV)	ζ_{i1}	(c_1)	ζ_{i2}	(c_2)
O	2s	−32.3	2.275			
	2p	−14.8	2.275			
Li	2s	−5.4	1.075			
	2p	−3.5	1.075			
Ti	4s	−8.97	1.075			
	4p	−5.4	1.075			
	3d	−10.81	4.550	0.4206	1.400	0.7839

[a] From *Table of Parameters for Extended Hückel Calculations*, collected by S. Alvarez, Barcelona, 1985. H_{ii}, orbital ionization energies; ζ_{ij}, Slater exponents; c_j, coefficients in the double-zeta expansion of d orbitals. Orbitals of Li are contracted to achieve reasonable overlap with O orbitals.

3. Crystal Structures

The basic structural unit of titanium oxide structures is the octahedron TiO_6,[2] where each Ti is hexacoordinated and the stoichiometry requires each O atom to be three-coordinated. For steric reasons there is not enough space for three independent octahedra to coordinate a single O atom, all TiO_2 structures must share edges of the octahedra. Many patterns of sharing are known in TiO_2 structures, the most simple one is encountered in rutile[42,43] where by the sharing of two opposite edges, linear chains of octahedra extended in the *c* direction are formed. The sharing of edges is always accompanied by a deformation of the octahedra. A typical feature is the shortening of four equatorial Ti−O bonds and the lengthening of two axial ones, and considerable distortion of bond angles, the pattern of which varies depending on the symmetry of the system.

Considerable efforts have been made in order to reach an understanding of the nature of the interactions behind deformation of the octahedra. Glassford and Chelikowsky[26] performed an extensive first principles study of the bonding in rutile. They successfully compared mechanical, electronic, and optical properties of the rutile structure of TiO_2 with experimental measurements, but the mechanism of interactions leading to the deformation of the octahedra was not revealed. Similar studies were described by Burdett, who used semiempirical tight-binding methods to describe the electronic control of geometry in rutile and related structures.[44] He performed many evaluations of energy contributions to the bonding in rutile structures. Neither of them led to a better understanding of the problem. He discussed also nonbonded Ti−Ti repulsions and the possible importance of the through-space mechanism relative to the through-bond mechanism, and pointed out similarities to deformations in SiO_2 structures.[45−47]

The cubic spinel $LiTi_2O_4$ contains eight formula units in the primitive unit cell reduced to two formula units in the face-centered unit cell (Figure 2a, left). The close-packed array of O atoms is located at the 32*e* positions of the space group $Fd\bar{3}m$. The Ti atoms occupy the half of the octahedral sites designated as 16*d*, while Li atoms occupy the eight tetragonal sites designated 8*a*. In this structure each structural unit TiO_6 shares six edges with surrounding units. The pattern of the sharing is indicated in Figure 2a (right) with thick lines. All three edges of one face are shared with three different units without sharing of faces. There are two variable parameters in the spinel structure: the lattice parameter *a* and an internal parameter *x*.

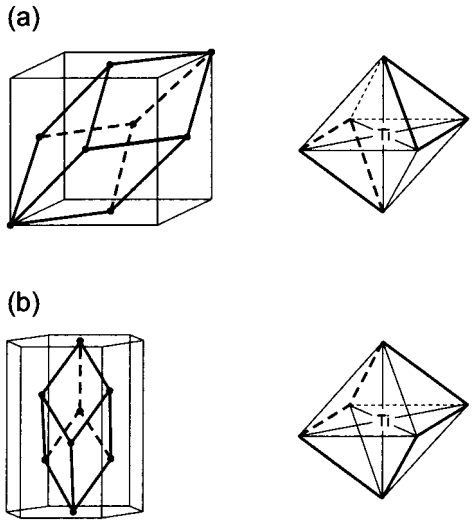

Figure 2. Unit cells of spinel and trigonal structures. (a) Primitive unit cell and the face-centered unit cell (left) and the pattern of sharing edges of the TiO_6 structural unit (right). (b) Hexagonal and rhombohedral unit cells (left) and the pattern of sharing edges in the layered structure (right).

The trigonal structure α-$NaFeO_2$ contains three formula units $LiTiO_2$ in the hexagonal unit cell and only one formula unit in the rhombohedral cell (Figure 2b, left). The Ti atoms reside in 3*a* positions of the space group $R\bar{3}m$ in planes of octahedral sites between the hexagonally stacked close-packed oxygen layers (6*c* positions). The Li atoms are located in the 3*b* positions and the Li and Ti atoms occupy alternate planes forming the layered structure (Figure 1). The pattern of edge sharing within the layered arrangement is indicated in Figure 2b (right). Because of symmetry requirements only three variable parameters are permitted: the lattice parameters *a* and *c* and an internal parameter *x*.

The structures of both compounds $LiTi_2O_4$ (spinel) and $LiTiO_2$ (trigonal) were fully optimized with respect to the variable parameters. These geometry parameters of the optimized structures are shown in Table 2, while the coordination spheres of the metal atoms are visualized in Figure 3. The deviation of the calculated spinel lattice parameter differs from the experimental value by less than 0.5%.[5] The TiO_6 octahedra are ideal, neither in the spinel nor in the trigonal structure. The deviation of angles from 90 degrees, however, is not as large as in simple oxides, such as rutile,[48] anatase,[49] and brookite.[50] For simple oxides the angle deformations are accompanied by a separation of the Ti−O bond lengths into at least two categories (e.g. four short and two long bonds in rutile). In both the spinel and trigonal structure the lengths of all Ti−O bonds remain unchanged for symmetry reasons (Table 2 and Figure 3). The angle deformations show a pattern similar to that in simple oxides. In all structures the O−Ti−O angle (for a couple

(41) Whangbo, M. H.; Evain, M.; Hughbanks, T.; Kertezs, M.; Wijeyesekera, S. D.; Wilker, C.; Zheng, C.; Hoffmann, R. *Extended Hückel Molecular and Crystal Calculations*; QCPE Program No. 571; Indiana University: Bloomington, IN, 1988.
(42) Abrahams, S. C.; Bernstein, J. L. *J. Chem. Phys.* **1971**, *55*, 3206.
(43) Restori, R.; Schwarzenbach, D.; Schneider, J. R. *Acta Crystallogr.* **1987**, *B43*, 251.
(44) Burdett, J. K. *Inorg. Chem.* **1985**, *24*, 2244.
(45) O'Keeffe, M. In *Structure and Bonding in Crystals*; O'Keeffe, M., Navrotsky, A., Eds.; Academic Press: New York, 1981.
(46) O'Keeffe, M.; Hyde, B. G. *Trans. Am. Crystallogr. Assoc.* **1979**, *15*, 65.
(47) Hyde, B. G.; O'Keeffe, M. *Nature (London)* **1984**, *309*, 411.
(48) Burdett, J. K.; Hughbanks, T.; Miller, G. J.; Richardson, J. W.; Smith, J. V. *J. Am. Chem. Soc.* **1987**, *109*, 3639.
(49) Howard, C. J.; Sabine, T. M.; Dickson, F. *Acta Crystallogr.* **1991**, *B47*, 462.
(50) Meagher, E. P.; Lager, G. A. *Canad. Miner.* **1979**, *17*, 77.

Table 2. Geometry Information on $LiTi_2O_4$ (Spinel) and $LiTiO_2$ (Trigonal) and Corresponding Li Deintercalated TiO_2 Structures; Available Experimental Values Are Supplied in Parentheses,[5] and Trigonal Structures Are Characterized in Hexagonal Axes

	space group	*a* (Å)	*c* (Å)	*z*	*V* (Å^3)	Ti−O (Å)	Ti−Ti (Å)	O−O (Å)	O−Ti−O (deg)
TiO_2	F*d*$\bar{3}$*m*	8.47	−	0.2664	607.6	1.99	3.00	2.61	81.7
$LiTi_2O_4$	F*d*$\bar{3}$*m*	8.45	−	0.2622	603.4	2.02	2.99	2.70	84.0
		(8.410)	−	(0.2622)	(594.8)	(2.005)	(2.973)	(2.683)	(84.0)
TiO_2	R$\bar{3}$*m*	2.99	14.2	0.265	36.65	1.94	2.99	2.60	82.9
$LiTiO_2$	R$\bar{3}$*m*	2.93	15.1	0.255	37.42	2.06	2.93	2.91	89.6

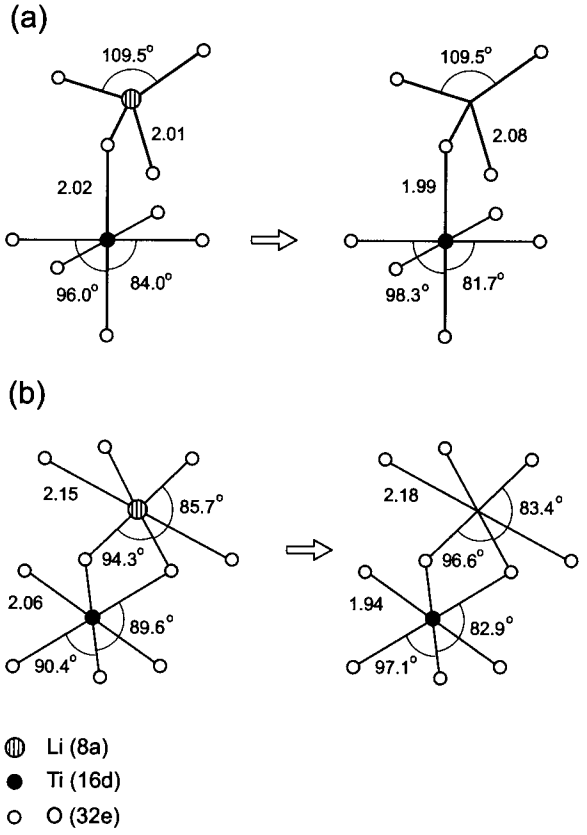

Figure 3. Geometry parameters of the coordination spheres of optimized structures: (a) spinel structure, (b) trigonal structure. Intercalated structures are shown on the left-hand side, deintercalated structures are shown on the right.

of oxygens shared by two octahedra) becomes smaller than a right angle. Such a deformation leads to a decreased O−O distance and increased Ti−Ti distance. All TiO_2 structures exhibit a stable electronic configuration of closed shells having no electronic reason for such a deformation. Possible explanations are available in terms of the atomic dimensions and nonbonding through-space interactions. Much larger Ti atoms do repel each other leading to increased Ti−Ti distances, while the much smaller dimensions of the O atoms allow them to get closer together (cf. discussions for rutile[44] and for SiO_2 structures[45−47]). From this point of view the Ti−Ti distance seems to be a crucial parameter for the stability of crystal structures containing edge-shared TiO_6 structural units. Within a series of TiO_2 oxides: rutile, anatase, and brookite, the stability increases and the values of the experimental Ti−Ti distance are 2.96, 3.04, and 3.06 Å, respectively. A comparison of Ti−Ti distances for the spinel and trigonal structure indicates higher stability of the spinel structure. This is in agreement with the fact that only the spinel structure was observed.[3−6] Data in Table 2 show that the structure of the layered trigonal $LiTiO_2$ is much more rigid than that of spinel $LiTi_2O_4$ (cf. O−Ti−O angles, Ti−Ti, and O−O distances). The packing in two dimensions probably prevents this structure from undergoing stabilizing deformations, which seems necessary for the Ti structures.

The effect of the deintercalation is similar in both structures. The interatomic distance between Ti and O is shortened and structures are more deformed. When lithium is not present, the Ti−O bonds become more polar. The oxygen atoms withdraw more electron density from the TMs and increase the positive charge on the Ti atoms. The repulsion between increased positive charges then yields more highly deformed structures. The Li atoms intercalated into TiO_2 structures then represent a counterbalance to the highly polar Ti−O bonds, thus leading to a more symmetrical arrangement of the lattice. The intercalation of Li causes the unit cell volume of the trigonal structure to be increased by 2.1% but curiously, that of the spinel structure is decreased by 0.7%.

4. Electronic Structure

Density of States. The total and partial DOS evaluated for optimized structures are shown in Figure 4 (spinel) and Figure 5 (trigonal). For the sake of comparison, all spectra are aligned in the way that the edges of the second band (from left) have zero energy. Figures 4 and 5 show that the DOS distribution is very similar in all compounds. In the valence region the energy states are collected in three main bands. The partial DOS projected to atomic orbitals, which are also displayed in Figures 4 and 5, show that they are—according to the dominant component—the s band, the p band, and the d band (the classification of bands is given at the top of Figure 4a).

Different width of bands reflect different bonding properties of states. An effective bonding is driven by two factors: orbital overlap and energy matching of interacting levels. A good energy matching and the large overlap produces the covalent bonding with an electron density considerably increased between the two atoms. The covalent bonding typically keeps the atoms at shorter distances. The dispersion of energy levels which are due to the covalent bonding is large and bands in the DOS representation are therefore wider compared to bands of ionic bands.[25] The bonding properties of states are in detail compared in the next paragraph based on the interaction scheme, which shows the energy matching, as well. Here we present the comparison of the width of bands in Figures 4 and 5.

The s band, situated at the left-hand side of each spectrum, consists mainly of O (2s) states. Its narrowness is an indication for the ionic character of these states. Small admixtures of orbitals from neighboring atoms (Ti and Li) and the fine structure of the band reveals some overlap and covalent mixing of electron densities residing in both O (2s) orbitals on one side, and Ti (3d), (4s), (4p) and Li (2s), (2p) on the other side. The p band with the O (2p) states as a dominant component is the main bonding band. According to the Ti (3d) admixture found in the band, its states originate from O (2p)−Ti (3d) interactions. The increased bonding character of these interactions, compared to the s band, is documented with bandwidths shown in Table 3. The values of bandwidths show that the covalency of the p bands is increased by at least a factor of ∼2.5 in all compounds.

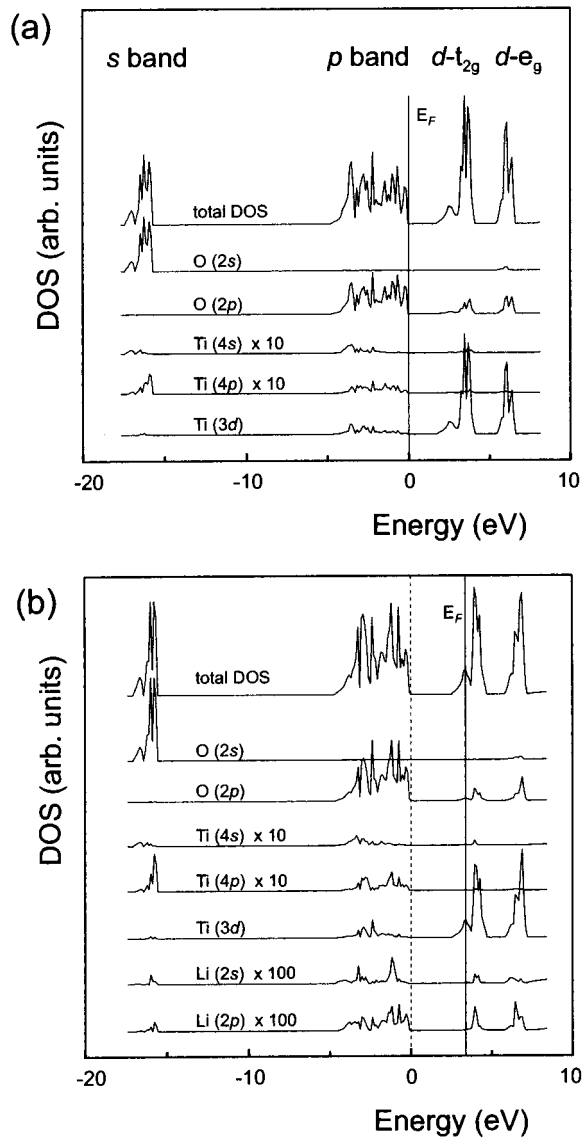

Figure 4. Total and partial density of states of spinel structures. (a) The Li extracted TiO_2 and (b) $LiTi_2O_4$. The assignment on the top of Figure 4a is valid for spectra in Figures 4 and 5.

In both deintercalated structures, the Fermi level (E_F) falls to the edge of the p band, as in other structure modifications of TiO_2. The d states situated at the right-hand side of the spectra are split into "t_{2g}" and "e_g" symmetry components due to the quasi-octahedral surrounding of the Ti atoms. They are separated from the p band by a gap of about 2 eV. The gap for spinel structures is located directly at the Γ point. Trigonal structures show indirect gaps. Although we used GGA functionals,[39] our calculated gaps are ∼33% lower than the experimental value,[27] which is ∼3.0 eV.

The intercalated Li atoms supply additional electron density that drives the location of E_F upward into the d band. Figure 4 shows that in spinels the d states are practically not affected by intercalation and Li electron density only increases upon filling of the bands of the host material. This means that for d bands of spinels, the rigid band model is valid. Possibly this is due to the fact that in the cubic spinel crystal lattice all deformations are proportionally balanced. The deformation of the Ti and Li coordination spheres in the trigonal structure (Figure 1b) causes remarkable changes in the electronic structure. Figure 5 shows that the intercalation of Li and subsequent relaxation of the

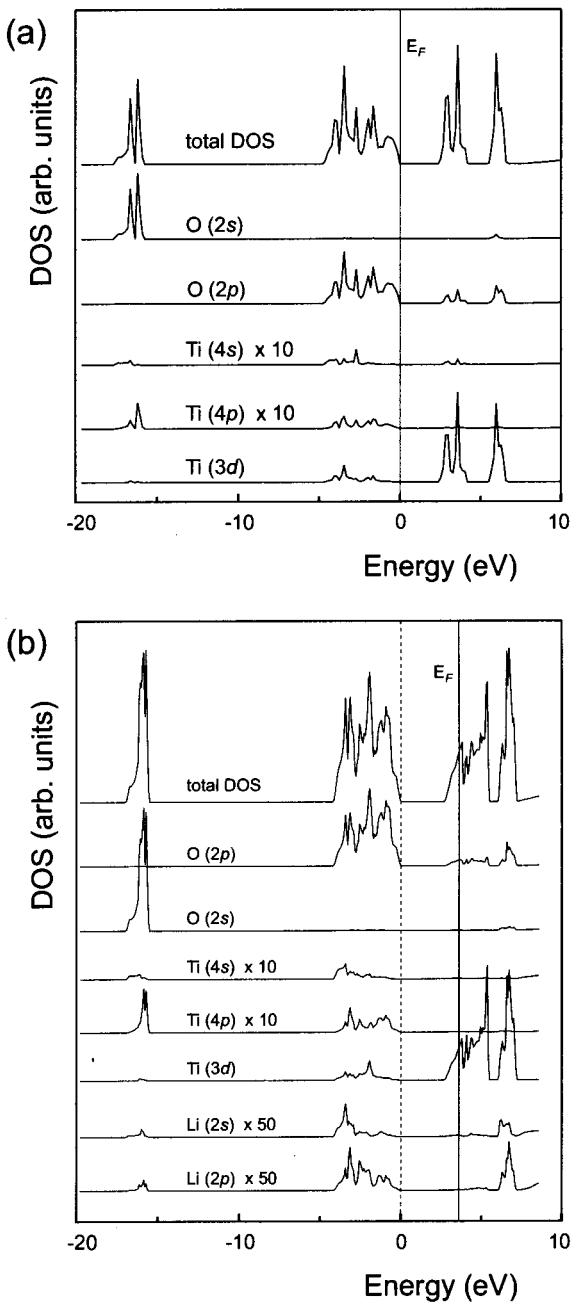

Figure 5. Total and partial density of states of trigonal structures: (a) Li-extracted TiO_2, (b) $LiTiO_2$.

Table 3. Widths of s and p Bands of $LiTi_2O_4$ (Spinel) and $LiTiO_2$ (Trigonal) and Corresponding Li Deintercalated TiO_2 Structures (in eV)

	TiO_2 (spinel)	$LiTi_2O_4$ (spinel)	TiO_2 (trigonal)	$LiTiO_2$ (trigonal)
s band	1.73	1.51	1.88	1.44
p band	4.73	4.63	4.74	4.20

structure induce some rearrangement of states at the bottom of the d band. The rigid band model, supposing no changes of the electronic structure, is therefore not valid. Note that Li intercalation causes a narrowing of both s and p occupied bands (Table 3). This means that the bonding within the host framework becomes more ionic upon Li intercalation.

Interaction Scheme. The construction of the interaction scheme for solids is a useful tool for presenting electronic structures of solid compounds in order to describe the basic features of "chemical" bonding.[51] The concept of the interaction

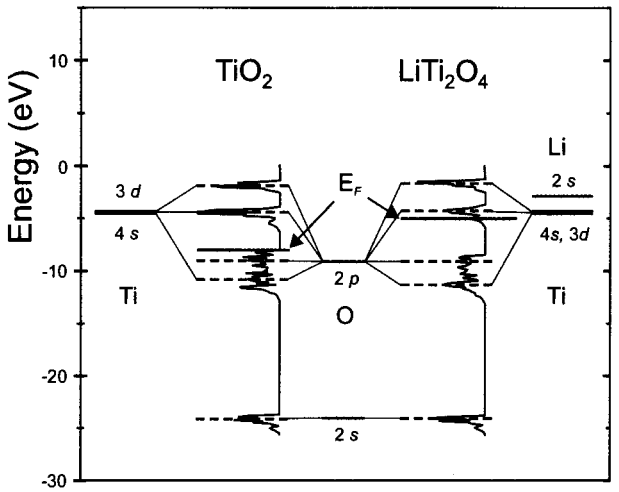

Figure 6. Interaction schemes compared for TiO_2 and $LiTiO_2$ in spinel structures.

scheme is based on the idea of putting the DOS on the absolute energy scale together with free-atom energy levels.[28−31,52] Figure 6 shows two such schemes constructed from our calculated DOS for the spinel structures TiO_2 and $LiTi_2O_4$. Atomic energy levels are calculated employing a scalar relativistic treatment[36] for the O ($2s^2$, $2p^4$) and Ti ($4s^2$, $3d^2$) configurations. The position of the DOS on the energy scale is usually calibrated using experimental ionization energies.[53,54] Because of the lack of experimental data for the inner valence shells of TiO_2[53,54] the DOS in Figure 6 are positioned by fitting of the calculated DOS to the free-atom O (2s) energy level. The states of the s band are all bonding, i.e. shifted to more negative energies. The stabilizing shift, however, is for the inner valce bands rather small. This was demonstrated for example for GaN[55] and for a series of semiconductors GaN, GaAs, GaP, which were calibrated using ionization energies of Ga (3d) nonbonding electrons. In the case of TiO_2 and $LiTi_2O_4$ (Figure 6) the DOS is positioned according to the upper part of the s band which is placed to the position similar to that of the free-atom O (2s) level.

The interaction scheme (Figure 6) instructively shows the relation of solid-state bands and the free-atom energy levels. Dashed lines within the DOS stand for mass centers of the bands. The basic information on bonding within the system comprises (i) orbital interactions, (ii) bonding properties of states, and (iii) covalency/ionicity relations of individual states. In Figure 6 the orbital interactions are indicated by interaction lines. They are identified according to the mixing of states originating from atoms which are the nearest neighbors (Ti and O). Partial DOS (Figures 4 and 5) show that the dominant interaction responsible for the shape of the DOS is the Ti (3d)−O (2p) interaction. This interaction shifts the most of corresponding states which are predominantly of p character toward positions, on the energy scale, which are more negative as compared with atomic levels. This is in agreement with the general notion of stabilizing energy levels through bonding. Two dashed lines within the p band symbolically indicate that states belonging to this band are of two kinds. Though the band is not divided into two subbands the admixture of Ti (3d) states indicates that the lower part of the band—i.e. the more stabile one—consists of states resulting from the Ti (3d)−O (2p) orbital interactions. These are the most covalent states of the system. The upper part of the band comprises only slight or no admixture of the Ti (3d) states. These states are slightly bonding or nearly nonbonding representing the electron density cumulated around the O atoms. Interaction lines therefore indicate orbital interactions only for the lower part of the band, and the states in the upper part all originate from the oxygen atoms. Note that the position of the upper subband is similar to that of the free-atom O (2p) level. The scheme shows that the position of the d bands is also driven by the Ti (3d)−O (2p) interaction. The partial DOS in Figures 4 and 5 indicate considerable admixture of p states into both d bands. Except for this p-to-d interaction there are no other relevant orbital interactions in the system.

In the interaction scheme the bonding properties of the different states are easily recognized. When states are placed in a stabilized position as compared to the corresponding atomic level—i.e., interaction lines are going down—the states are bonding. In both compounds states belonging to the p band are typically bonding. States of the deeper lying s band are also bonding but stabilized to a much lesser extent. The d bands are divided into an antibonding component (e_g) which is destabilized as compared to the position of the free-atom 3d level, and a nonbonding one (t_{2g}) with a subband of slightly stabilized states.

The covalency/ionicity relations of individual states are indicated by several features:

(a) Covalent states are formed by mixing of electron densities from at least two centers, i.e. such states are found in the scheme according to orbital interactions indicated by interaction lines. A certain degree of covalency could be therefore expected only for states in the lower part of the p band and in the d band. The electron density corresponding to the upper part of the p band corresponds to the nonbonding interactions. Because of the small admixtures to the s band, no interaction line is drawn toward the Ti-centered orbitals and therefore very small covalency could be expected for the states of the s band.

(b) Covalent states result from orbital interactions between levels (orbitals) having similar electronegativities. In the interaction scheme the difference in electronegativities is apparent from the energy difference between interacting atomic levels (ΔE). A large value of the ΔE indicates a large difference in electronegativities. Interaction schemes in Figure 6 show that due to the large value of $\Delta E_{pd} = 4.8$ eV even the most covalent states in the bottom part of the p band are rather ionic. From this point of view the states in the s band with a value of $\Delta E_{sd} = 14.7$ eV are typically ionic taking part mainly in electrostatic interactions.

(c) Bands due to covalent interactions are always broader than those due to more ionic interactions.[51] As already discussed above, the Ti (3d)−O (2p) bonding in $LiTi_2O_4$ is more ionic because its p band is considerably narrower than that of the corresponding TiO_2 structure. From these arguments it is clear that the shape of the DOS is driven by covalent interactions, while ionic interactions can only cause a shift of the energy levels but no modification of the DOS envelope.

As pointed out several times the width of a band is an indicator of the covalency/ionicity of bonding. The width, however, strongly depends on the interatomic distance and on the overlap between orbitals. The following question therefore emerges: "What is the relation of the covalency/ionicity and interatomic distances?" Because in covalent bonding there is

(51) Hoffmann, R. *Solids and Surfaces: A Chemist's View of Bonding in Extended Structures*; VCH: New York, 1988.
(52) Benco, Ľ. *Chem. Papers* **1997**, *51*, 129.
(53) Carlson, T. A. *Photoelectron and Auger Spectroscopy*; Plenum: New York, 1978.
(54) Nefedov, V. I. *X-ray Photoelectron Spectroscopy of Solid Surfaces*; VSP: Utrecht, 1988.
(55) Dudešek, P.; Benco, Ľ.; Daul, C.; Schwarz, K. *J. Phys.: Condens. Matter* **1998**, *10*, 7155.

always an increase of the electron density between the atoms, let us consider the magnitude of this increase as a criterion of the degree of covalency. If one expands, e.g. a diamond lattice, bonding remains covalent, but the degree of covalency decreases and the bands become narrower. At a very large expansion of lattice atoms do not feel each other and energy bands recover to free-atom energy levels. Because of extremal narrowness of bands and spherical distribution of the electron density, free atoms are typical ionic centers. From this point of view the lengthening of a bond and the increase of the ionicity are the two sides of the same story.

For the spinel structures the DOS envelopes displayed in Figures 4 and 6 are very similar especially at the bottom of the d band where the additional electron density from the Li atoms is accommodated. This makes an impression that the rigid-band model is valid and there is no change of the shape of the total DOS and no change of covalency/ionicity of bonding. The change of the bandwidth presented in Table 3, however, proves the nonvalidity of the rigid-band model for the intercalation of Li into TiO_2 structures.

Another feature which is apparent from the interaction scheme is the transfer of the Li electron density. In their recent papers Ceder et al.[23,24] argue on the basis of first principles calculations, in contradiction to the common belief of charge-transfer from Li to the TM, that a substantial part of the electron density of Li is transferred to the oxygen atoms. The interaction scheme shows that all O bonding states within the p band are occupied. The electron density supplied by the intercalated Li atoms can fill only the lowest unoccupied states, which are available at the bottom of the d−t_{2g} band. It is true that these states admix some p character. This occurs because the admixture of the d states to the p band raises a corresponding part of the p states into the d band. The bottom of the d band is certainly dominated by d states with small admixture of p states (cf. partial DOS in Figure 4b). The filling of these states therefore cannot cause substantial charge transfer to the O atoms.

Population Analysis. Bonding properties of states are in Figure 7 displayed by means of crystal orbital overlap populations (COOP). These are calculated for spinel structures TiO_2 and $LiTi_2O_4$ to complement the analysis presented above in terms of the interaction scheme. The COOP curves are calculated for the LAPW optimized geometries of both TiO_2 (a) and $LiTi_2O_4$ (b), using extended Hückel tight binding semiempirical method.[41] I the upper part of Figures 7a and b the total and partial DOS are given for reference. Comparison of DOS from first-principles (Figures 4 and 5) and those in Figure 7 shows that width of bands and energy gaps of semiempirical DOS are rather unrealistic. The width of the p band is too small and the gap separating the s and the p bands is too large. The picture of the bonding, however, is correct and analysis of bonding properties of states allows a better interpretation of the results.

The COOP curves, displayed for Ti−O, O−O, and Ti−Ti pairs of atoms, show similar bonding pattern in both compounds. States due to Ti-to-O interactions are all bonding up to the upper edge of the p band. Within the d band the negative values indicate antibonding character of Ti-to-O interactions. Note decreased COOP curve for the upper part of the p band showing nonbonding character of these states. Second-neighbor O-to-O and Ti-to-Ti interactions are, because of smaller overlap, much weaker than the interaction of nearest-neighbors Ti and O. Within the s and p band the COOP curves show both bonding and antibonding character of the O-to-O interaction proving that this interaction contributes to the broadening of bands of

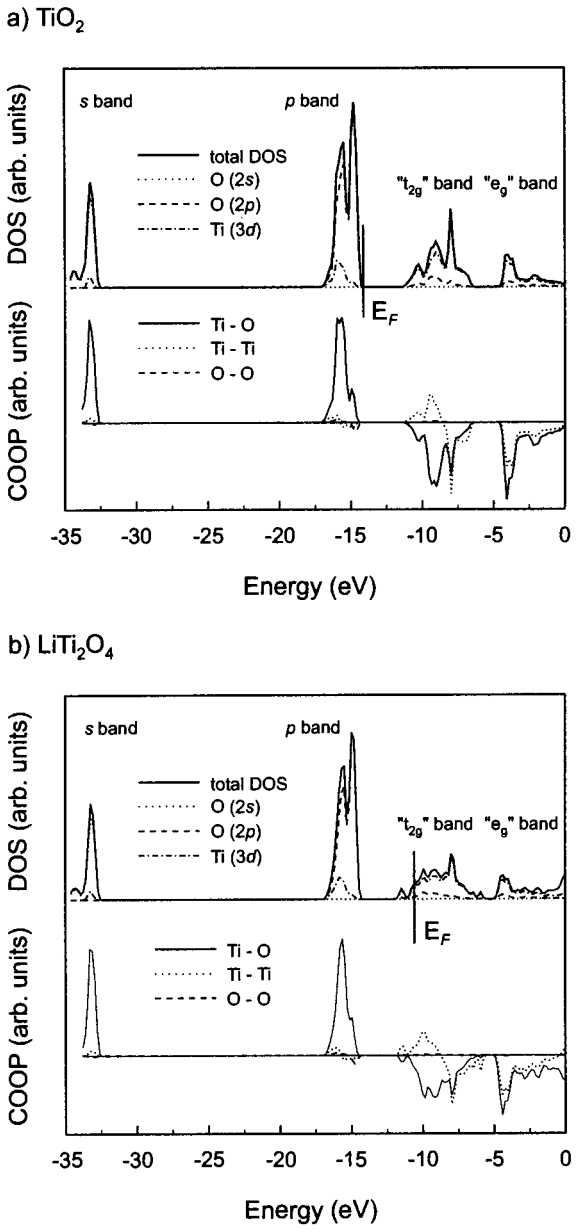

Figure 7. COOP curves for Ti−O, O−O, and T−Ti interactions in TiO_2 (a) and $LiTi_2O_4$ (b) spinel structures. The total and partial DOS displayed in the upper part of both figures are given for reference.

occupied states. A dominant feature of the Ti-to-Ti interaction is pronounced bonding character of the states situated in the lower part of the t_{2g} band. It is similar in both compounds and appears because of considerable overlap of Ti-t_{2g} orbitals. While in TiO_2 these metal-to-metal bonding states are empty (cf. position of the Fermi level in Figure 7a), in $LiTi_2O_4$ a fraction of these states is occupied (Figure 7b). This means that in the Li intercalated structures the metal-to-metal interactions increase the stability of the system.

The bonding properties of states, presented in terms of the COOP curves in Figure 7, are in good agreement with the analysis of bonding in terms of the interaction schemes presented in Figure 6. The advantage of the COOP curves is that they easily show bonding of second-neighbors. The interaction scheme, contrary, provides good understanding of bonding of the nearest-neighbors.

Electron Density. Figure 8 shows electron densities displayed for spinel structures. Two kinds of evaluations are performed.

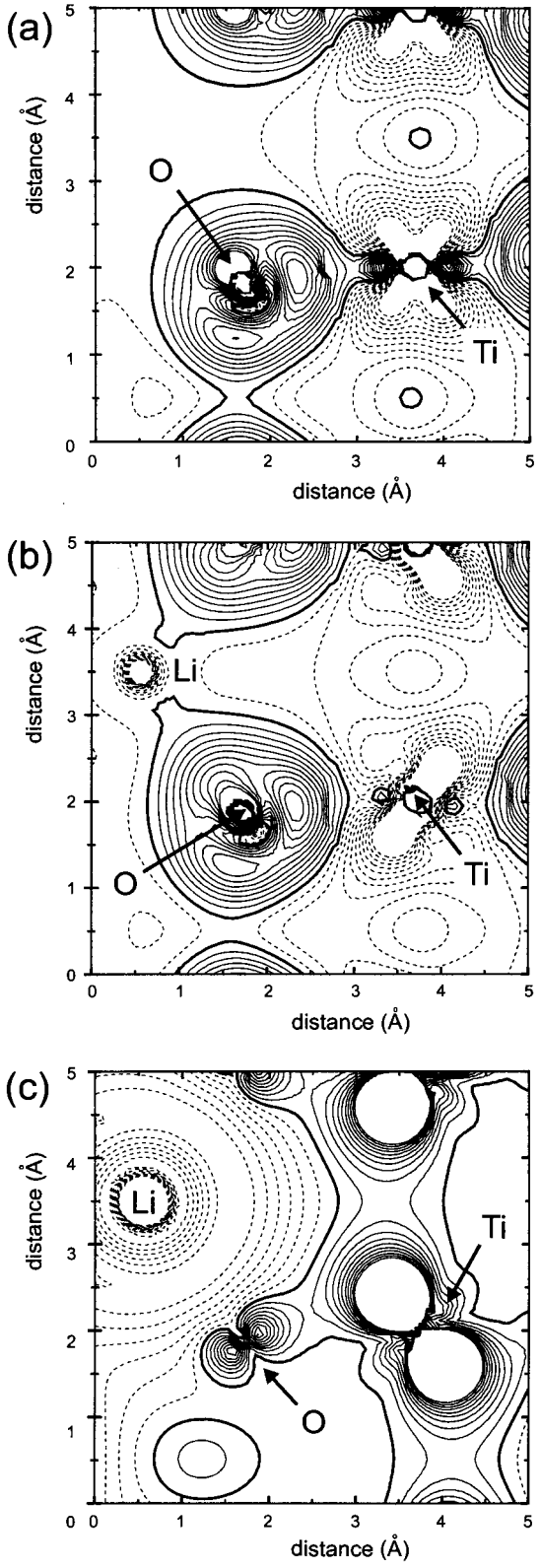

Figure 8. Difference electron densities within the (110) plane of the spinel structure. (a) Difference map constructed from all valence densities of TiO_2. (b) Difference map of $LiTi_2O_4$. (c) Difference map constructed of Li electron density. Continuous, thick continuous, and dashed lines indicate positive, zero, and negative values, respectively. Contour spacings are 0.02 e/Å^3 (a and b) and 0.005 e/Å^3 (c).

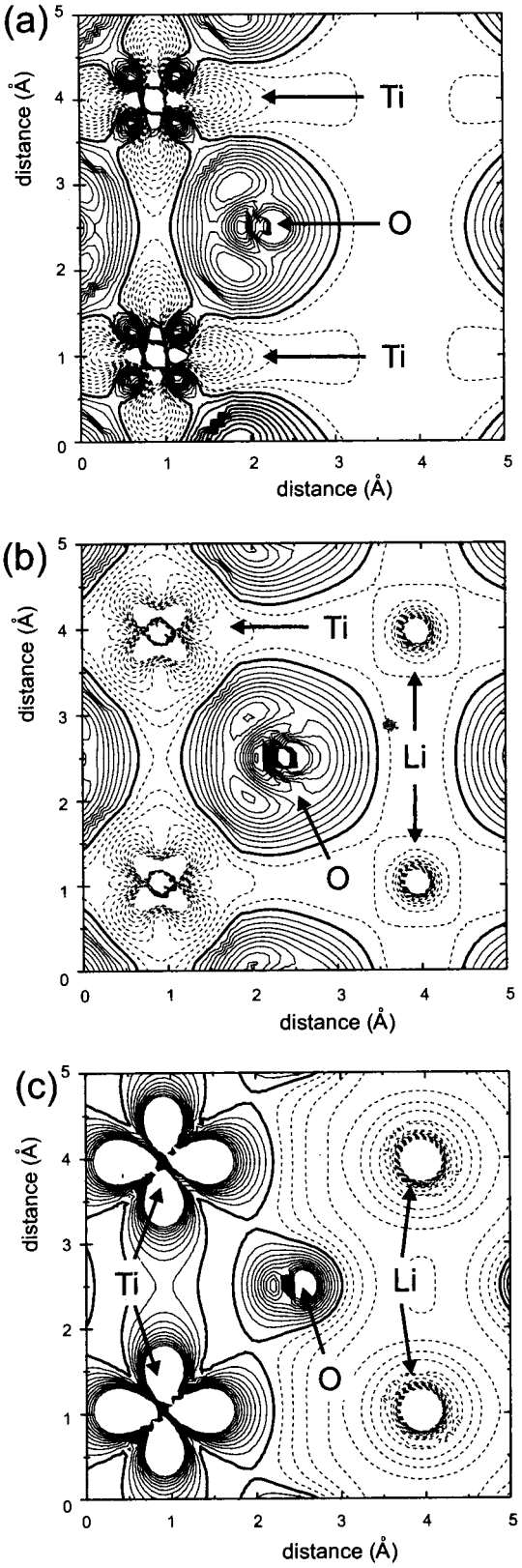

Figure 9. Difference electron density within the (211) plane of the trigonal structure. (a), (b), and (c) as in Figure 8. Contour spacings are 0.02 e/Å^3 (a and b) and 0.01 e/Å^3 (c).

First we display the difference electron valence density (DEVD) averaged over the whole valence region for both the deintercalated and the intercalated compound. Second, for the intercalated compound we display the difference electron band-density (DEBD) constructed only from the Li electron density. Figure 8a displays the DEVD for the (110) plane (diagonal cut of the unit cell) showing the effect of bonding on the electron density of free atoms. The bonding electron density is confined

on O atoms in a rather spherical manner, but showing some directional dependence. The TM sites are depleted of electron density. The depletion is rather symmetric and its shape indicates that electrons are withdrawn mainly from the d (t_{2g}) orbitals. There is also some increase of the electron density on Ti atoms in the direction toward the O atoms. This increase is due to the covalent interaction of O (2p) with Ti (e_g) orbitals. This participation in the bonding pushes the remaining e_g states upward as the antibonding counterpart, while t_{2g} orbitals remain rather nonbonding. Figure 8b shows the effect of the Li electron density on bonding. The increased density on oxygen atoms is similar to that in deintercalated compounds and does not seem to be remarkably influenced by the intercalation. The Li sites are completely depleted. The shape of contours on Ti atoms shows that the electron density is transferred to the TMs. They still show lack of electron density as compared to that in free atoms, but it is now partially compensated by the density from Li atoms. An important feature in this figure is the fact that after the intercalation of Li the covalent O (2p)−Ti (3d) bonding is considerably diminished. This is in line with the decrease of the width of both bonding bands discussed above. In Figure 8c the difference density is only evaluated in the cutting plane for Li electron density in the d band. It shows the depletion of the Li sites and the transfer of electron density to the TM, where it fills t_{2g} orbitals. Some minor part of the electron density is transferred also to the O atom, and its shape shows that this contributes to the bonding toward the d (t_{2g}) orbitals. The spacing of the contour lines is chosen in such a way as to stress the large difference between the amount of electron density transferred to the TM and O atoms. In the spinel structure the electron density supplied during the intercalation of Li in fact builds up the metal-to-metal bonds of t_{2g}−t_{2g} type within the host framework. The area of increased electron density in the lower left part of Figure 8c indicates another chain of the Ti−Ti bonds oriented perpendicular to the projection plane. Because of the cubic symmetry, three such independent chains of Ti−Ti bonds are allowed to extend in all three dimensions. The build up of this 3D network of effective metal-to-metal bonds explains why the spinel structure does not expand, but slightly shrinks upon intercalation of Li, and also explains the good stability of spinel $LiTi_2O_4$ compounds.[6,57] This network, which is composed of degenerate t_{2g}-like orbitals, represents the electronic foundation of superconductivity observed in $LiTi_2O_4$ monocrystals.[6,57] The Li atoms serve as a source of the ionic, i.e. easily transferable, electron density. The transfer of electron density to the TM atoms enables the formation of the Ti−Ti network and the superconductivity of stoichiometric $LiTi_2O_4$. The introduction of Li deficiencies into the structure causes a local decrease of E_F and thus a breaking up of the Ti−Ti network leading to the loss of superconductivity.[57] Figure 9 shows electron density plots analogous to those in Figure 8. They are evaluated in the (211) projection plane of the trigonal structure of $LiTiO_2$, containing the Li and the O atoms of the equatorial plane of TiO_6 octahedra. The electron density plots exhibit most of the features described for the spinel structure in Figure 8. The DEVD in Figure 9a shows the sizable depletion of the t_{2g} electron density and the formation of a certain covalency between Ti (e_g) and O (2p) orbitals. In the intercalated compound the features of covalency are lost (Figure 9b). The DEBD displayed in Figure 9c shows again that most of the Li electron density is transferred to the Ti atoms. The small fraction of electron density transferred to the O atom increases the antibonding interaction between O and Ti within the projection plane just opposite to the spinel structure where this interaction is bonding. The emergence of the Ti−Ti network is even stronger in the trigonal structure as compared to that in spinels. This network is again composed of Ti (t_{2g}) orbitals. Note that the e_g orbitals are those pointing toward the O atoms. For symmetry reasons the metal-to-metal bonds, however, form only linear chains.

5. Conclusions

The comparison of the calculated electronic properties of optimized structures of Li intercalated and Li deintercalated compounds shows the validity and limitations of the rigid band model for the spinel and trigonal lattices. Both the DOS and the interaction scheme show that a transfer of Li electron density is possible only to the TM atoms. Both analysis of the DOS and of the electron densities show that the Li intercalation decreases the covalency of the host TiO_2 framework. A moderate and symmetry-balanced relaxation of the cubic structure accompanied by only a slight change of the unit cell volume and by the formation of the 3D network of metal-to-metal connections are probably the reasons why only the spinel structure is observed experimentally. At the end of the TM series the smaller size of the TM d orbitals probably prohibits the creation of effective 3D metal-to-metal networks, therefore, layered trigonal structures become more stable which are then strengthened by the linear metal-to-metal chains formed upon intercalation of Li atoms.

Acknowledgment. This work was supported by the Swiss Federal Office of Energy. We thank L. Smrcok for assistance with retrievieng structural data, P. Blaha for numerous discussions on the computer code WIEN97, and K. Müller for helpful suggestions. Special thanks to one anonymous reviewer who pointed out the role of the s-to-s and p-to-p covalent interactions.

IC9803558

(56) Campá, J. A.; Vélez, M.; Cascales, C.; Gutiérrez Puebla, E.; Monge, M. A.; Rasines, I.; Ruíz Valero, C. *Physica* **1994**, *C235*, 749.
(57) Moshopoulou, E.; Bordet, P.; Sulpice, A.; Capponi, J. J. *Physica* **1994**, *C235*, 747.